

Phthalimides: Supramolecular Interactions in Crystals, Hypersensitive Solution ^1H -NMR Dynamics and Energy Transfer to Europium(III) and Terbium(III) States

Robertha C. Howell ¹, Selvin H. Edwards ¹, Alison S. Gajadhar-Plummer ¹, Ishenkumba A. Kahwa ^{*1}, Gary L. McPherson ², Joel T. Mague ², Andrew J. P. White ³ and David J. Williams ³

¹ Department of Chemistry, University of the West Indies, Mona Campus, Kingston 7, Jamaica, West Indies.

² Department of Chemistry, Tulane University, New Orleans, Louisiana 70118, USA.

³ Chemical Crystallography Laboratory, Department of Chemistry, Imperial College of Science, Technology and Medicine, South Kensington, London SW7 2AY, United Kingdom

* Author to whom correspondence should be addressed; Tel +1-(876) 927 1910; Fax +1-(876) 977 1835; E-mail: ikahwa@uwimona.edu.jm

Received: 7 December 2002; in revised form: 26 June 2003 / Accepted: 27 June 2003 / Published: 15 July 2003

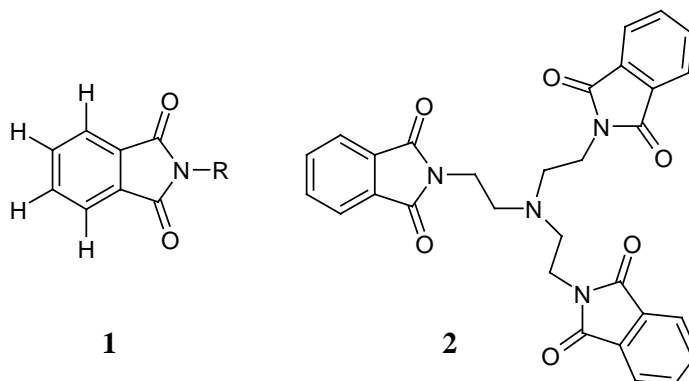
Abstract: Detailed crystal structures and ^1H -NMR characteristics of some alkylamine-phthalimides, including dendritic polyphthalimides, are reported. These investigations were undertaken in order to obtain a better understanding of the relationship between solid-state supramolecular interactions, their persistence in solution and associated dynamics of magnetically hypersensitive phthalimide aromatic AA'BB'-AA'XX' proton NMR resonances. Some alkylamine phthalimides feature folded molecular geometries, which we attribute to n- π interactions among proximal amine-phthalimide sites; those alkylamine-phthalimides that have no possibility for such interactions feature fully extended phthalimide functionalities. Accordingly, alkylamine phthalimide compounds with folded solid-state geometries feature solvent and temperature dependent hypersensitive AA'BB'-AA'XX' ^1H -NMR line profiles, which we attribute to the n- π interactions. Luminescence of $\text{Eu}^{3+}({}^5\text{D}_0)$ and $\text{Tb}^{3+}({}^5\text{D}_4)$ states show well defined metal

ion environments in their complexes with dendritic phthalimides, as well as relatively weak phthalimide-lanthanide(III) interactions.

Keywords: Phthalimides, n - π interactions, dynamic NMR chemical shifts, lanthanides luminescence.

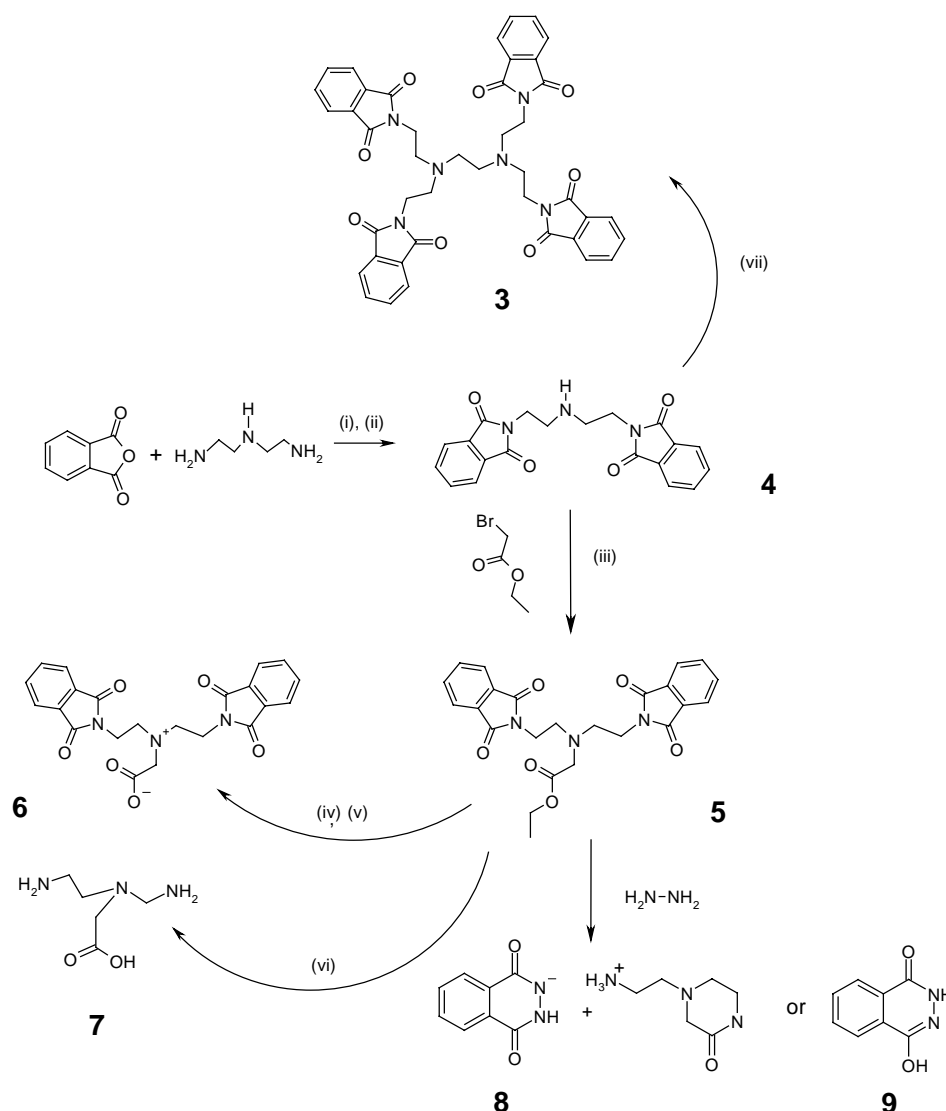
Introduction

Phthalimide moieties (**1**) have the propensity to engage in solid-state n - π , π - π , dipole-dipole and other supramolecular interactions, depending on the detailed nature of the proximal functional groups [1-3]. In one case, **2**, where the solid-state structure featured the phthalimide functionality in active n - π interactions with a proximal tertiary amine site, spectacular solvent and temperature dependent second order [4] aromatic ^1H -NMR spectral profiles were obtained [1]. It was therefore tentatively proposed that the n - π interaction between a phthalimide group and a proximal tertiary amine is also active in solution and that for **2** all the three phthalimide groups are involved in the dynamic interaction. Thus, the n - π interactions were deemed crucial events in the process by which magnetic hypersensitivity of the phthalimide protons is triggered [1]. However, no other examples of phthalimides which exhibit such solid-state n - π interactions and corresponding hypersensitive second order solution ^1H -NMR spectral profiles have been reported.

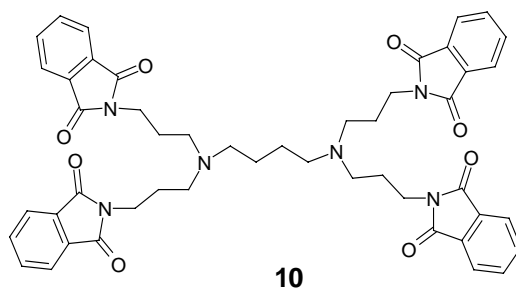
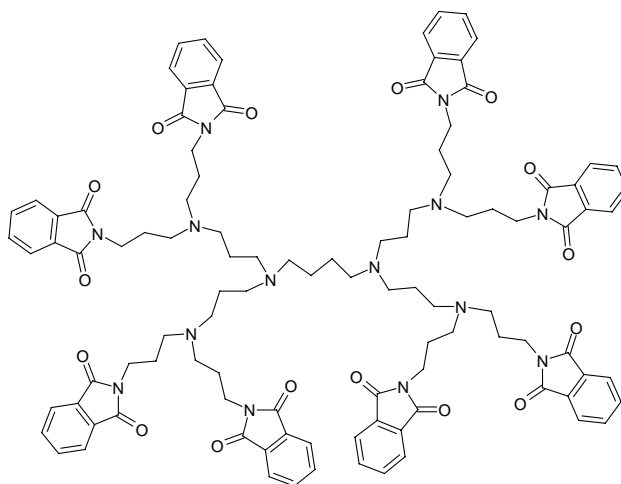
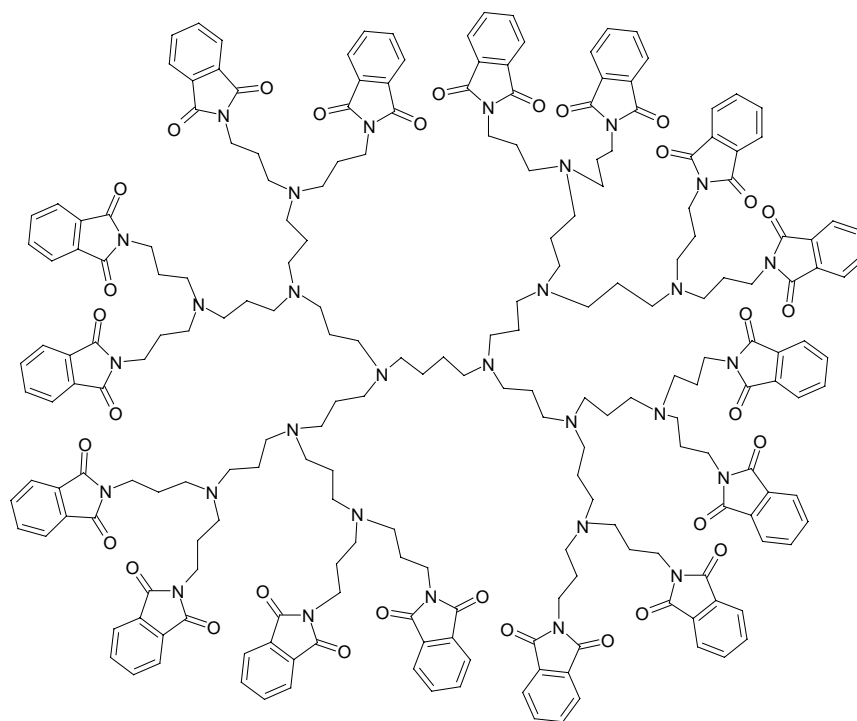


While factors governing the magnetic susceptibility dynamics that are responsible for the spectacular ^1H -NMR line profiles are still obscure, the potential of such profiles to provide insights into supramolecular interactions [1], in which the phthalimide moiety so readily engages [1-3, 5-9], is of great interest. For these reasons, preparation and detailed structural characterization of new examples of phthalimides with potential to exhibit solid state n - π interactions that are accompanied by hypersensitive solution ^1H -NMR spectral profiles were undertaken. Because of our ongoing interest in phthalimides as protecting groups in the syntheses of alkyl polyamino acids such as **7** [1-3] and dendritic analogues, we sought to prepare and study the solid state structures and solution NMR behavior of di-phthalimides **5** and **6** (Scheme 1) and dendrimers **3** and **10-12**. Polyamino acids such as **7** are desirable starting materials in the development of new types of luminescent [10-16] and

paramagnetic [17-21] biomedical diagnostics. Like **2**, compounds **5**, **6** and dendrimers **3** and **10-12** feature tertiary amine sites with potential to engage in $n-\pi$ interactions with proximal phthalimide groups. Dendrimer **3** features a tertiary amine site across an ethylene linkage while the tertiary amine sites of dendrimers **10-12** are across longer propylene chains. It was interesting to determine how any differences in phthalimide - tertiary amine proximity would influence the $n-\pi$ interaction and, in turn, the $^1\text{H-NMR}$ spectral profiles of the phthalimide protons. Herein we report the preparation, crystal structures and supramolecular interactions of compounds **3**, **5**, **6**· H_2O , **8**· H_2O , **9** and $[\text{H}_2\text{10}][\text{ClO}_4]_2\cdot\text{CH}_3\text{CN}$, detailed $^1\text{H-NMR}$ behaviors of **3** and **5** and preliminary results on luminescence characteristics of europium(III) and terbium(III) complexes of dendrimers **10-11**.



Scheme 1. Compounds of interest and their preparation routes: (i) refluxing acetic acid (1 hour) [1-3]; (ii) ethanol and sodium carbonate (iii) potassium carbonate and refluxing toluene (2); (iv) $\text{NaOH}/\text{H}_2\text{O}/\text{Ethanol}$; (v) $\text{H}_2\text{O}/\text{HCl}$; (vi) details under development for a future report; (vii) dibromoethane, K_2CO_3 , 5 days refluxing in acetonitrile.

**10****11****12**

Results and Discussion

Compounds 5 and 6

Compounds **5** and **6** are readily prepared according to Scheme 1 (see Experimental section). The persistence of dimeric species in the FAB MS spectra of **5** is indicative of the presence of relatively strong intermolecular interactions [4]. Compound **6** does not experience aggregation in the FAB MS environment. To determine the presence and nature of supramolecular interactions [22] in compounds **5** and **6** single crystal X-ray studies were undertaken. The X-ray structure of compound **5** (Figure 1) shows the molecule to have a folded geometry, with one of the phthalimide units lying over the other and inclined by *ca.* 46° with respect to it.

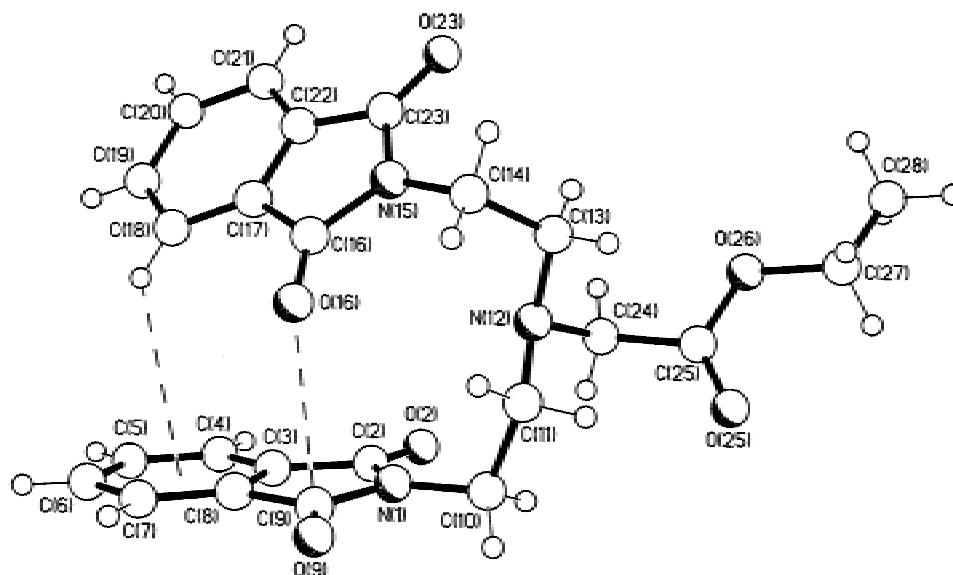


Figure 1. The molecular structure of compound **5** showing its folded geometry

One of the carbonyl oxygens [C(16)] of one phthalimide unit is positioned above and is orthogonal with respect to one of the carbon atoms [C(9)] of the other at a distance of 2.95 Å, resulting in intramolecular carbonyl-carbonyl electrostatic stabilization. This interaction is supplemented by a secondary weak C-H... π interaction between the C(18) hydrogen atom of one phthalimide unit and the C₆H₄ of the other (H... π , 3.06 Å, H... π vector inclined by 81° to the ring plane). Consistent with FAB MS behavior, pairs of molecules of **5** pack with a significant π ... π overlap between centrosymmetrically related phthalimide units (inter-planar separation 3.30 Å, ring centroid...ring centroid distance of 3.74 Å) (Figure 2).

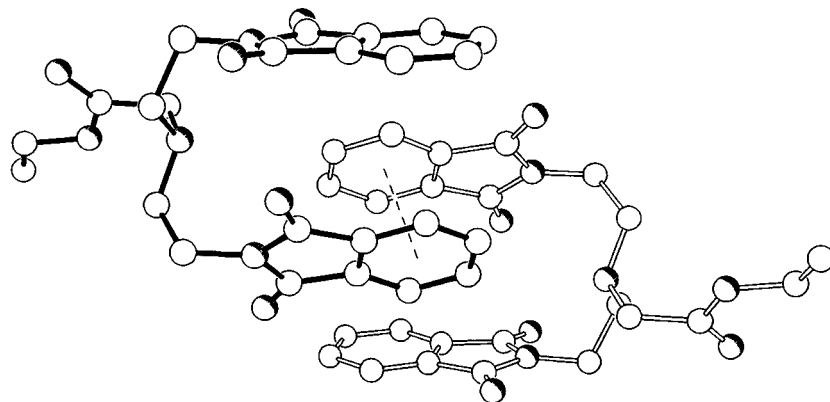


Figure 2: Intermolecular phthalimide-phthalimide π - π interactions stabilizing the **5** dimer

The structure of amino acid **6** (Figure 3) shows the molecule to have crystallographic C_s symmetry, while the $^+\text{NH}(\text{CH}_2\text{COO}^-)$ unit is on the crystallographic mirror plane. There is evidence that the carboxylic acid part is disordered across the mirror plane. Unfortunately it was not possible to resolve this disorder. The pattern of bonding in the phthalimide functionality is normal [1-3]. The unambiguous location of a H-atom on the tertiary amino center shows that the molecule exists in its zwitterionic form. Without the possibility for n - π interactions, the phthalimide arms of compound **6** adopt an all trans-geometry (compare with the folded geometry of **5** in Figure 1).

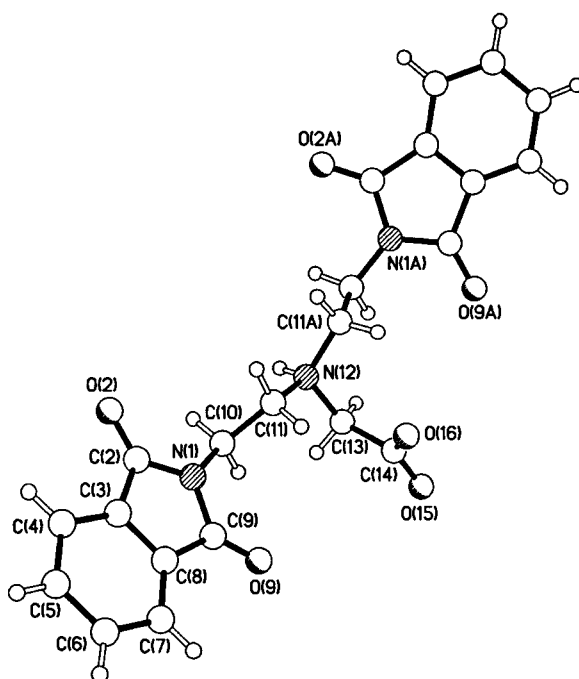


Figure 3: The molecular structure of zwitterionic phthalimide **6**.

Adjacent molecules are linked via N-H...O H-bonds between the ammonium group of one molecule and the carboxylate of the next etc. etc. (N...O), (H...O); 2.64, 1.77 Å; (N-H...O angle = 161°, Figure 4). This hydrogen bonded ribbon is further stabilized via a weak carbonyl...carbonyl interaction (3.2 Å) between C(9) in one molecule and O(2) in the next. Adjacent C_i related ribbons are weakly π -stacked (mean interplanar separation = 3.45 Å), the aromatic rings of the phthalimide units in one ribbon partially overlaying those in the next. The partial occupancy water molecules H-bond to each other and the carboxylate oxygen atom not already involved in H-bonding. Other intramolecular parameters in **5** and **6** compare well with previous determinations on similar functionalities [1-3].

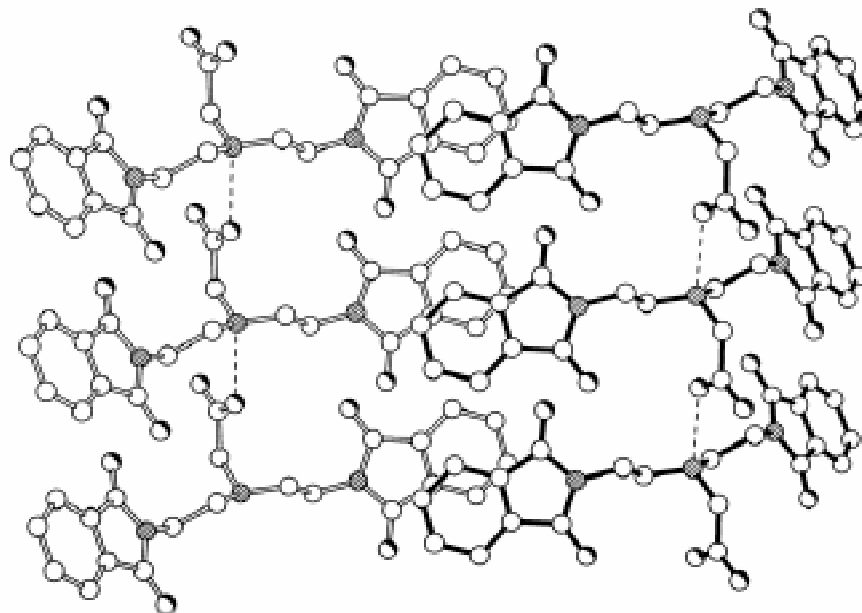


Figure 4. The supramolecular structure of **6** showing stabilizing phthalimide-phthalimide π - π and N-H...O hydrogen bonding interactions.

Reaction of 7 with Hydrazine

Because of our interest in the preparation of amino acid **7**, we explored the transformation of ester **5** into **7** using hydrazine [23]. The X-ray analyses of the crystalline reaction product of diphtalimide ester **5** with ethanolic hydrazine revealed the formation of a salt (**8**) comprised of a 4-ethylammonium piperazine-2-one lactam, phthalhydrazide mono-anion and a water molecule (Figure 5).

The FAB MS of product **8**, which features peaks at $m/z = 144$ (4-ethylammonium piperazine-2-one lactam), 166 (phthalhydrazide) and 287 (dimerized 4-ethylammonium piperazine-2-one), supports the formulation. Formation of piperazine-2-one moieties from proximal polyamines and esters is not unusual [24] but the phthalhydrazide mono-anion product is interesting and this is the first structural report on it. The pattern of bonding in the piperazine-2-one moiety is unexceptional while that in the phthalhydrazide anion exhibits marked asymmetric delocalization in the two amide components. The relative lengthening of the C=O bond in the anionic amide (1.284(2) Å) is significantly greater than in

the protonated one (1.261(2) Å), the former being accomplished by a noticeable increase in C=N double bond character (1.317(3) Å) cf. 1.336(2) Å for the protonated species. All potential donors and acceptors are involved in H-bonding interactions and these are supplemented by π - π stacking between C_i related phthalhydrazide anions to form stepped layers (Supplementary material Figure S1) that are oriented perpendicular to the crystallographic c -direction.

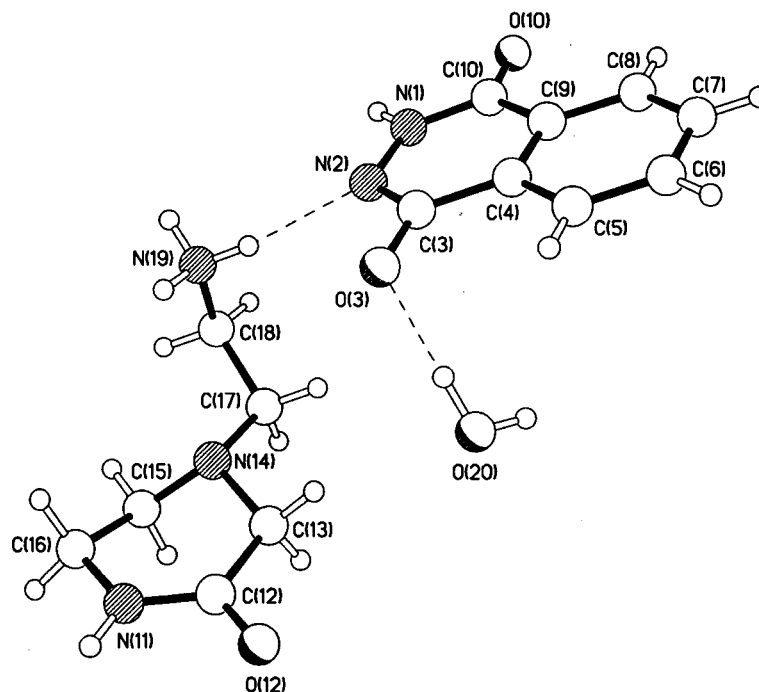


Figure 5: The asymmetric unit of compound **8**.

The only other possible ‘acceptor site’ that has not been utilized is the tertiary nitrogen on the piperazine moiety, which is shielded from approach by the terminal alkyl ammonium group.

With excess hydrazine (twice the amount used for **8**), compound **9** is obtained. The X-ray structure (Table 1 and Figure 6) reveals the formation of a hydrogen bonded trimer comprised of 3 crystallographically independent hydroxyl imine units (**9**) having nearly C_3 symmetry.

Table 1: Hydrogen bond geometries of **9** are respectively:

Bond	[X...Y] (Å)	[H...Y] (Å)	[X-H...Y] (°)
a	2.85	1.96	173
b	2.84	1.94	177
c	2.84	1.95	170
d	2.68	1.79	171
e	2.68	1.78	167
f	2.68	1.78	175

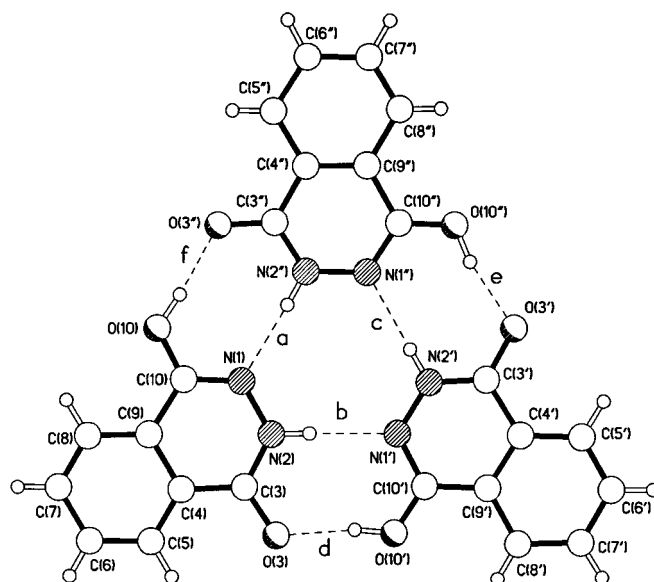
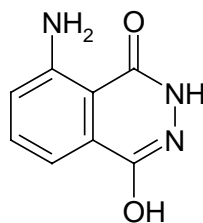


Figure 6: The hydrogen-bonding-stabilized trimeric structure of compound **9**

The pattern of H-bonding is identical to that observed in the closely related amino substituted analogue, luminol (**13**) [25]. There is one more (phenyl substituted) hydroxyl imine analogue the structure of which was reported recently [26].



13

In the present structure unambiguous location of all hydrogen atoms established the space group to be *Cc* rather than *C2/c* which requires there to be a C_2 axis passing through the bisectors of the $C(6')$ - $C(7')$ and $N(1')$ - $N(2')$ bonds. The approximation in the crystal symmetry is very close and is only broken by the O-H and N-H hydrogen atoms. Consequently, correlation effects are large and the accuracy of the bond lengths limited. The over all pattern of bonding in the amide and hydroxy imine is directly comparable with that observed in luminol (**13**). Although there are small out of plane twists of each molecule with respect to each other, the over all assembly is essentially planar with a maximum deviation of *ca.* 0.25 Å. The hydrogen bonded trimers are arranged head to tail to form 'ribbons' that run along the crystallographic *b* direction and are π -stacked (Supplementary material Figure S2) with *c*-glide related ribbons (mean interplanar separation *ca.* 3.4 Å).

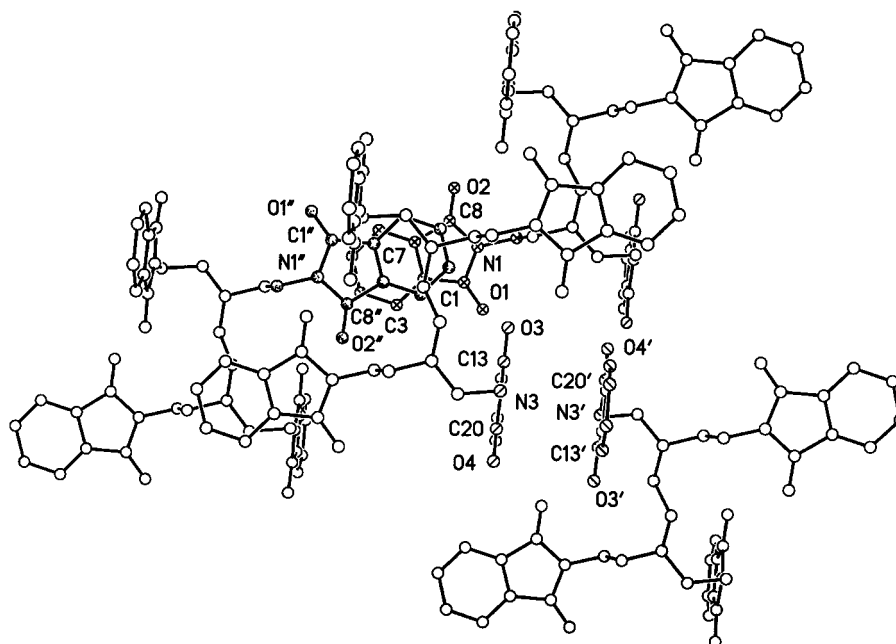


Figure 8: A portion of the supramolecular structure of **3** with the two independent sites (N1 and N3) for $\pi \dots \pi$ stacking highlighted.

At the same time, the phthalimido group containing N1 participates in a somewhat weaker π -stacking interaction with its counterpart in the molecule at $-x, 1-y, 1-z$. Here the mean interplanar spacing is 3.634(4) Å and the details of the stacking are shown in the Supplementary material Figures S3 and S4. Pertinent interatomic distances are: C2---C6'' = 3.635(3), C2---C7'' = 3.818(3), C5---N1'' = 3.744(3), C5---C1'' = 3.784(3), C7---C3'' = 3.860(3), C8---C4'' = 3.642(3) Å. The short C-O distances (1.205(3) – 1.207(2) Å) indicate that the carbonyl groups are not significantly conjugated with the remainder of the phthalimido group while the C-N distances in this unit (1.386(2) – 1.390(2) Å) are significantly shorter than a single C(sp²) – N(sp²) bond (1.42 Å) [27] indicating partial double bond character. Both of these features have been found previously in **2** and in other related compounds [1-4].

Elemental analyses were satisfactory for dendrimers **10** and **11** while **12** had large amounts of trapped potassium carbonate and phthalic acid. However, the presence of these dendrimers in the preparations was indicated [28] by FAB MS for **10** (m/z; calc. for H**10**⁺, 837; obs., 837) and **11** (m/z; calc. for H**11**⁺, 1814; obs. 1814) and Matrix-Assisted Laser Desorption Ionization (MALDI) for **12** which featured a peak at m/z = 3800 due to [H**12**·2H₂O]⁺ (calc. m/z = 3802). However, dendrimers **10**-**12** were difficult to obtain in single crystal X-ray diffraction quality form; we thus attempted to isolate them as hydrogen salts but this was successful for only [H₂**10**]²⁺, which was confirmed by single crystal X-ray diffraction analyses of [H₂**10**][ClO₄]₂·CH₃CN (Figure 9).

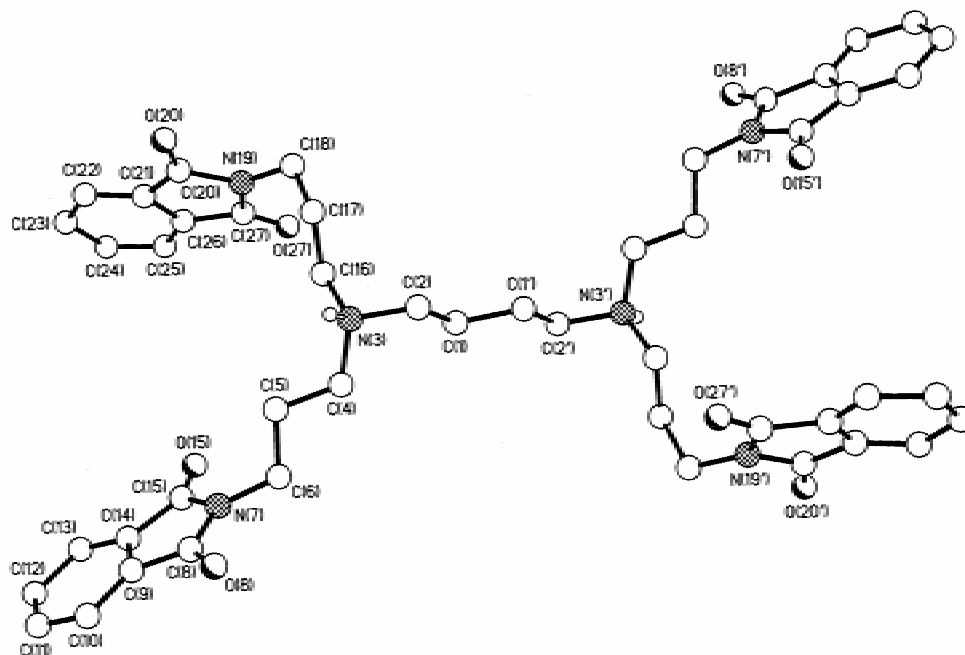


Figure 9: The structure of the $[\text{H}_2\mathbf{10}]^{2+}$ cation.

Consistent with the presence of protons on the tertiary amine sites, no folding of the phthalimide arms similar to that exhibited by **2**, **3** and **5** is featured by $[\text{H}_2\mathbf{10}]^{2+}$. However, as for other phthalimides, extensive π - π stacking interactions among the phthalimide moieties dominate the supramolecular array of $[\text{H}_2\mathbf{10}][\text{ClO}_4]_2 \cdot \text{CH}_3\text{CN}$ (Supplementary material Figure S5).

The above crystal structure studies revealed that compounds **3** and **5** featured the n - π interaction characterized by a prominent folding of the phthalimide arms towards the tertiary amine site (Figure 7 for **3** and Figure 1 for **5**). The detailed NMR behaviors of compounds **3** and **5**, were thus sought to determine whether these solid state n - π bonding features could produce the kind of spectacular solvent and temperature evolutions of the phthalimide ^1H -NMR spectral profiles similar to those exhibited by **2** [1].

*Hypersensitive ^1H -NMR of **3** and **5***

The ^1H -NMR spectrum of **3** features one very prominent second order pattern for the aromatic protons which possesses approximate mirror symmetry (Figure 10) and is similar to that exhibited by the aromatic protons of compound **2** [1]. The observed single second order pattern for the aromatic ^1H resonances means that in solution the four phthalimide moieties are equivalent on the time scale of the NMR experiment. Since there are two tertiary amine sites and four phthalimide functionalities in **3**, the very prominent single set of second order aromatic ^1H resonances suggests that the four phthalimide groups are engaged in dynamic n - π interactions with the two tertiary amine sites – a behavior very much similar to that of **2** [1].

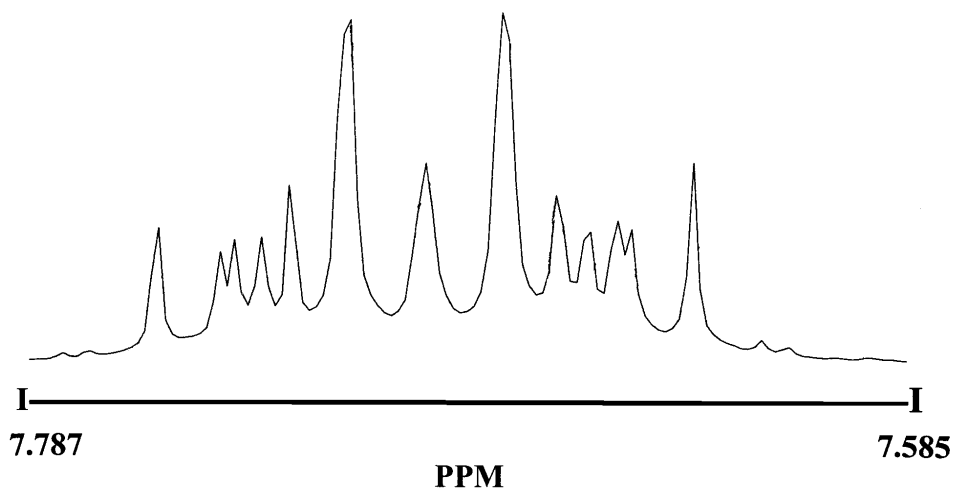


Figure 10: The hypersensitive second order $^1\text{H-NMR}$ resonances of phthalimide groups of **3** in Cl_3CD at room temperature

Dendrimers **10** - **12**, which also possess lone pairs on tertiary amine sites proximal to the phthalimide functionality, feature somewhat similar second order $^1\text{H-NMR}$ behavior. For example, dendrimer **11** features a pair of well separated phthalimide AA' -BB' resonances in CDCl_3 (7.8 - 8.2 p.p.m.) while **10** - **12** exhibit narrow singlets in $(\text{CD}_3)_2\text{SO}$ at about 7.8 p.p.m.

As observed for tris-phthalimide **2** [1] as well as dendrimers **3** and **10** - **12**, the $^1\text{H-NMR}$ chemical shifts and line profiles for the aromatic protons of compound **5** exhibit the strange hypersensitive behavior the evolution of which is dependent on the nature of the solvent and its temperature. For example, at 283 K the aromatic protons of compound **5** in CDCl_3 feature a singlet at *ca.* 7.67 p.p.m. while a pair of well-resolved quartets is found at *ca.* 7.74 and 7.62 p.p.m. with **5** in CD_3CN (Figure 11) or at *ca.* 7.68 and 7.57 p.p.m. for CD_3OD . Since the peaks are narrow, a dynamic regime dominates [1, 29] the fast (on NMR experimental time scale) process by which the second order aromatic proton resonance line profile transforms among a variety of AA'BB' and AA'XX' patterns. The equilibrium constant (K) for the process can be related to the resonance shifts using the equation developed earlier [1, 29]:

$$\ln\{(\delta_u - \delta)/(\delta - \delta_l)\} = \ln K = \Delta H^\# / RT - \Delta S^\# / R \dots\dots \quad (\text{eq. 1})$$

Where: δ_u = upper chemical shift limit;

δ_l = lower chemical shift limit;

δ = temperature dependent chemical shift of hypersensitive reference peak (the most intense one);

$\Delta H^\#$ = Process enthalpy;

$\Delta S^\#$ = Process entropy

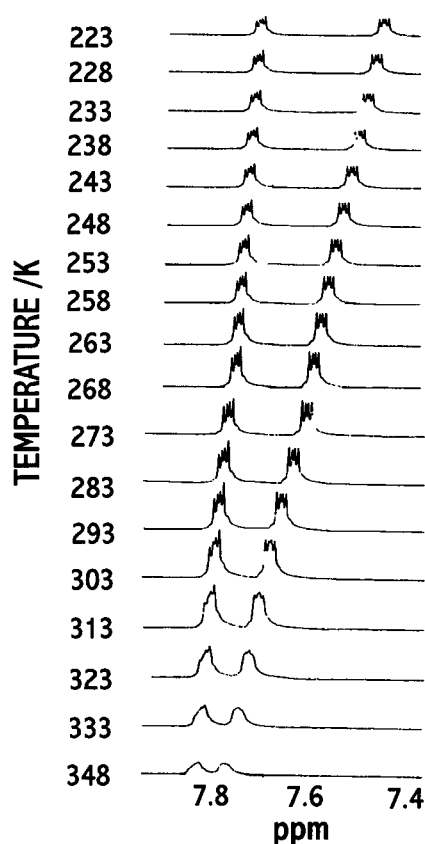


Figure 11. The temperature evolution of the phthalimide ^1H -NMR profile of **5** in CD_3CN . Sample spinning was stopped at high temperature ($T > 303\text{K}$) hence peak broadening.

As for **2**, the upper (δ_u) and lower (δ_l) limits of the temperature dependent resonance was not reached [1]. For comparative purposes the values of δ at the lowest and highest temperatures reached were used in place of δ_l and δ_u respectively; values of δ too close to limits so adopted were not used. Plots of $\ln K$ vs $1/T$ are given in Figure 12 for **5** in CD_3CN , CD_3OD and CDCl_3 and ΔH^\ddagger values derived from these plots are 23 ± 1 , 17 ± 3 and 19 ± 5 kJ/mol respectively. These values are very similar to those found (*ca.* 20 kJ/mol) for tris-phthalimide **2** in acetone and methanol [1].

Interestingly, the N-CH_2 ^1H (singlet) resonance of the $\text{N-CH}_2\text{COO}$ group of **5** is also hypersensitive; the protons are de-shielded and shifted to lower field as the temperature decreases (Supplementary materials Figure S6) and $|\Delta H^\ddagger| = 22 \pm 1$ kJ/mol. Indeed, the molecular structure shows these two protons to be oriented towards the same side as the tertiary amine lone pair in crystals of **5** (Figure 1), which should make them more susceptible to effects of the n - π tertiary amine-phthalimide interactions. Consistent with this interpretation, the N-CH_2 protons of the two $\text{N-CH}_2\text{CH}_2\text{O}$ ($\text{O} =$ phthalimide) arms oriented away from the lone pair (Figure 1) are, as expected, not temperature dependent. Of course there is no guarantee that the solid state and solution structures of **5** are identical. Nevertheless, when all of the above observations are taken together, they provide preponderant

evidence in support of the dynamics of n- π tertiary amine-phthalimide interactions as the source of the observed hypersensitivity of aromatic ^1H magnetic susceptibility.

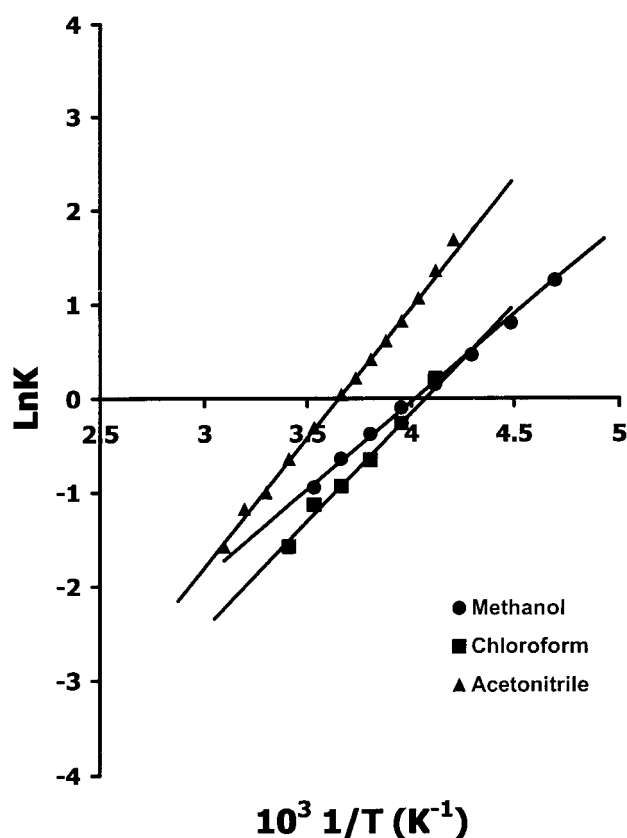


Figure 12: The evolution of $\ln\{(\delta_u - \delta)/(\delta - \delta_l)\}$ (i.e. $\ln K$) with temperature ($1/T$, K^{-1}) for **5** in CD_3Cl , CD_3CN and CD_3OD .

Luminescence of Europium(III) and Terbium(III) complexes of Dendrimer **10**

Luminescence from lanthanide(III) ions, especially europium(III) and terbium(III), is a good probe for electronic environments of organic chromophores with oxygenated coordination sites [30, 31]. For this reason we investigated chemical interactions between lanthanide(III) ions and dendrimers **10** – **12** which have enough phthalimide to facilitate metal ion complexation. Well defined stoichiometries for lanthanide(III) complexes with dendrimers **10** and **11** were obtained (see experimental sections) but clearly, crystals of X-ray diffraction quality are needed to resolve the stoichiometry issue and facilitate meaningful luminescence studies [32]. Nevertheless, results of preliminary luminescence studies of polycrystalline lanthanide(III) complexes of dendrimers **10** and **11** are similar; both feature broad photoemission, which have good spectral overlaps with europium(III) and terbium(III) electronic absorptions. Indeed, the excitation spectra for Eu^{3+} ($^5\text{D}_0 \rightarrow ^5\text{F}_j$) (Fig 13C) and Tb^{3+} ($^5\text{D}_4 \rightarrow ^5\text{F}_j$) ($j = 0 - 6$) (Figure 14C) emissions (Figures 13B and 14B respectively) feature dominant broad dendrimer

absorptions similar to those exhibited by the gadolinium(III) complexes (not shown). However, the narrow terbium(III) (Figure 14B) and europium(III) (Figure 13B) emissions are also accompanied by broad emission from ligand based states, which indicates that quenching of dendrimer emission by the Ln^{3+} ions (especially Eu^{3+}) is inefficient. This indicates that interaction between the lanthanide(III) ions and the phthalimide functionality is weak, a conclusion supported by luminescence decay curves which feature prominently slow excitation build-ups of ca. 2×10^4 and $6 \times 10^4 \text{ s}^{-1}$ for Eu^{3+} (${}^5\text{D}_0 \rightarrow {}^5\text{F}_j$) (Figure 13A) and Tb^{3+} (${}^5\text{D}_4 \rightarrow {}^5\text{F}_j$) ($j = 0 - 6$) (Figure 14A) respectively. The Eu^{3+} (${}^5\text{D}_0$) emission decay behavior is temperature dependent and not single exponential (fast components being $7 \times 10^3 \text{ s}^{-1}$ at 297 K and $2 \times 10^3 \text{ s}^{-1}$ at 77 K while slow components are $2 \times 10^3 \text{ s}^{-1}$ and $8 \times 10^2 \text{ s}^{-1}$ respectively). Tb^{3+} (${}^5\text{D}_4$) emission decay is temperature independent and single exponential ($1.5 \times 10^3 \text{ s}^{-1}$ at both 77 and 297 K).

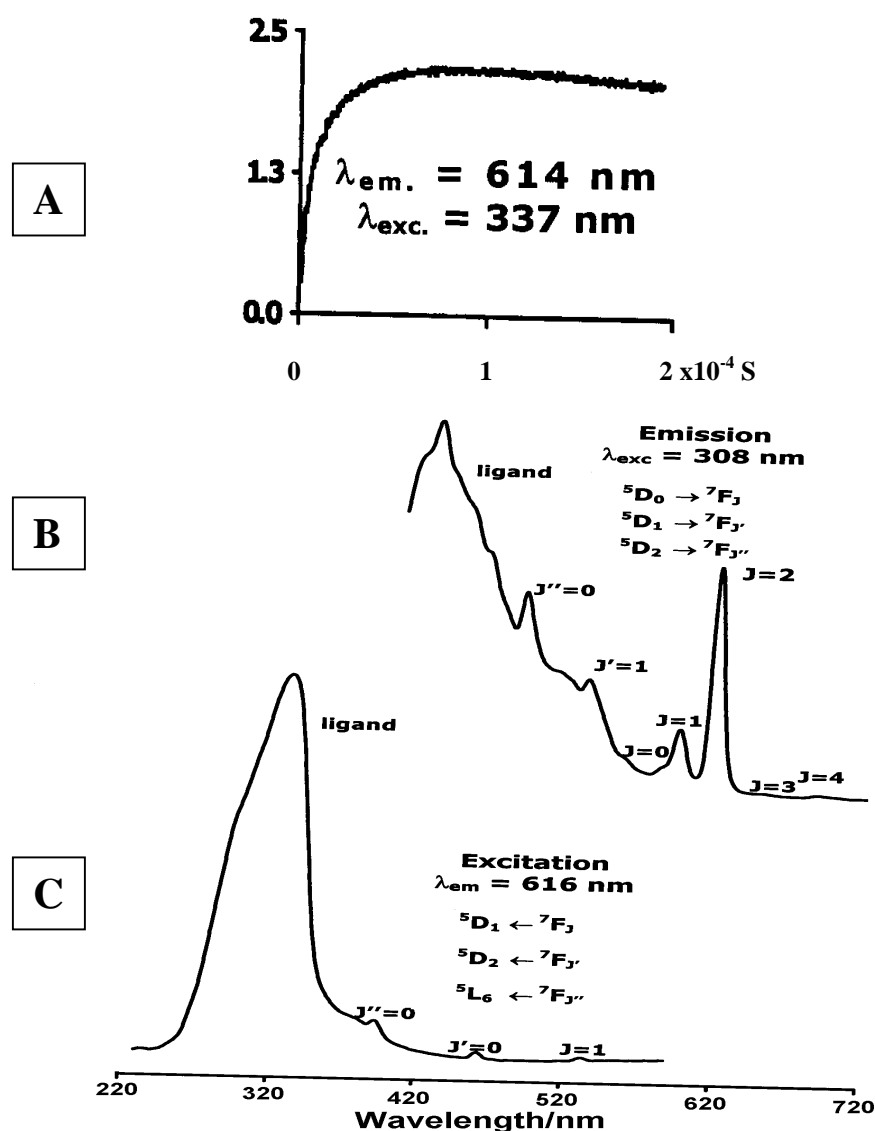


Figure 13. Luminescence of $\text{Eu}(\mathbf{10})(\text{NO}_3)_3$ at 77 K. (A) Slow Eu^{3+} (${}^5\text{D}_0$) excitation build-up following excitation of states of **10** at 337 nm; (B) Emission spectrum; (C) Excitation spectrum dominated by broad absorptions of **10**.

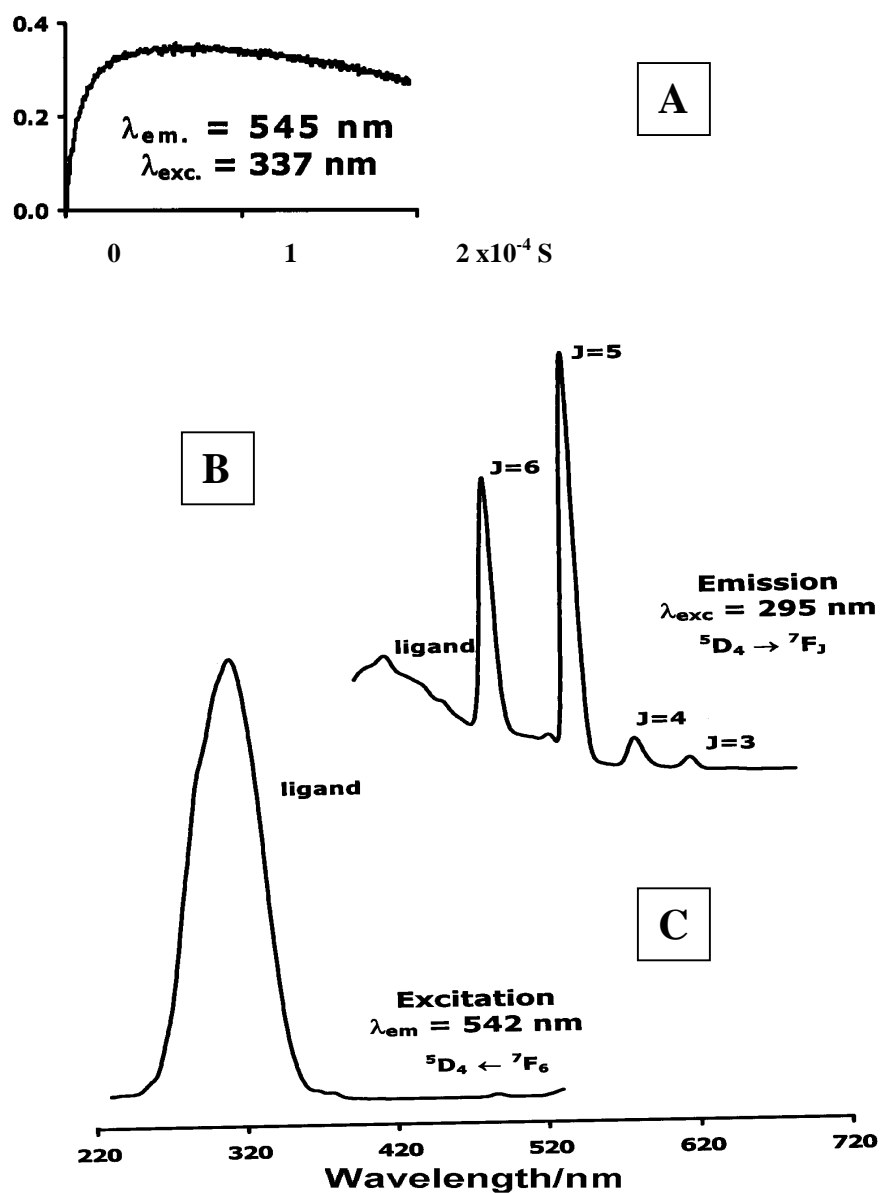


Figure 14. Luminescence of $\text{Tb}(\mathbf{10})(\text{NO}_3)_3 \cdot \text{HNO}_3$ at 77 K. (A) Slow $\text{Tb}^{3+}({}^5\text{D}_4)$ excitation build-up following excitation of states of **10** at 337 nm; (B) luminescence spectrum; (C) excitation spectrum dominated by broad absorptions of **10**.

Concluding Remarks

The crystal structures (Figures 1-9 and Supplementary material Figures S1-S5) of **3**, **5**, **6**· H_2O , **8**· H_2O , **9** and $[\text{H}\mathbf{10}][\text{ClO}_4]_2 \cdot \text{CH}_3\text{CN}$ show the propensity for the phthalimide and related phthalhydrazide functionalities to engage in a variety of non-covalent interactions leading to extended supramolecular aggregations. Compounds **3** and **5**, which like **2** have tertiary amine sites interacting

with proximal phthalimide functionalities, adopt a folded conformation similar to that of **2** [1]. By contrast, the zwitterionic compound **6** and dication $H_2\mathbf{10}^{2+}$, the tertiary amine site of which are protonated and thus unavailable for n- π interaction with the proximal phthalimide group, adopts an all trans-conformation in which the phthalimide groups are as far apart as possible. The presence of a tertiary amine site is thus an essential factor for the folded geometry of **2**, **3** and **5**. Correspondingly as in **2**, compounds **3** and **5** feature hypersensitive temperature and solvent dependent second order aromatic 1H -NMR line profiles. The temperature dependence of the 1H -NMR of the NCH_2COO group of **5** and the similarity of the magnitude of its process enthalpy (Eq.1) with that of the hypersensitive phthalimide 1H -NMR resonances, provide preponderant support for n- π interaction as the origin of hypersensitivity of phthalimide 1H -NMR resonances. While it is prudent not to use structural behaviors of small dendrimers such **2**, **3** and $H_2\mathbf{10}^{2+}$ as a basis for generalizations on structures of large dendrimers, results herein described point to a potentially important role of supramolecular interactions in determining the solid state geometry of a dendrimer. These factors must be considered along with spatial, steric and molecular gyration behavior [33] in modeling physical and chemical properties of dendrimers [34]. The significance of some of these supramolecular factors has been discussed recently [35].

Acknowledgements

We thank the Leverhulme Trust (project F/709) and the Inter-American Development Bank-UWI development program for supporting the work at UWI. We also thank the National Science Foundation and Louisiana Board of Regents (LEQSF) (Tulane-UWI) and the British Council (Imperial College-UWI) for supporting our collaborations.

Experimental

General

Materials (purity, source): Ethylbromoacetate (98%, Aldrich); acetic acid (BDH); dendritic amines **10** -**12** used to make dendritic phthalimides (95%, DSM Fine Chemicals); lanthanide sesquioxides (99.99%, Aldrich); phthalic anhydride (GPR, BDH); hydrazine (over 99%, BDH); dibromoethane (OR, Mallinckrodt).

Analyses: Carbon, hydrogen and nitrogen analyses were obtained from MEDAC Ltd., Brunel University, Uxbridge UK. Positive ion FAB MS analyses were done using AutoSpecQ spectrometer and m-NBA matrix. Isotopic abundance patterns were calculated using the programs available freely at Sheffield University web-site: [http://www.chem.schef.ac.uk/webelements.cgi\\$ isot](http://www.chem.schef.ac.uk/webelements.cgi$ isot). IR spectra were recorded using a Perkin Elmer 1600 series FT-IR spectrometer, while NMR spectra were recorded using a AC200 MHz Brüker at UWI or 400 and 500 MHz spectrometers from General Electric at

Tulane University. The equipment setup used to obtain luminescence spectra and lifetimes was described earlier [21].

Crystallography

Table 2 provides a summary of crystallographic data, data collection and refinement parameters for compounds **3**, **5**, **6**·H₂O, **8**·H₂O, **9** and [H₂**10**][ClO₄]₂·CH₃CN. Data for **5**, **6**·H₂O, **8**·H₂O, **9** and [H₂**10**][ClO₄]₂·CH₃CN were collected on Siemens P4/PC diffractometers using ω -scans, whilst those for **3** were collected on an Enraf-Nonius CAD-4 diffractometer using $\theta/2\theta$ -scans. The structures were solved by direct methods and they were refined using full-matrix least-squares based on F^2 . The polarity of **9** could not be unambiguously determined. All crystallographic data (excluding structure factors) have been deposited with the Cambridge Crystallographic Centre. CCDC176542-176547 contains the supplementary crystallographic data for this paper. These data can be obtained free of charge via www.ccdc.cam.ac.uk/conts/retrieving.html (or from the CCDC, 12 Union Road, Cambridge CB2 1EZ, UK; fax: +44 1223 336033; e-mail: deposit@ccdc.cam.ac.uk).

Table 2: Essential crystallographic data for compounds **3**, **5**, **6**·H₂O, **9** and [H₂**10**][ClO₄]₂·CH₃CN

Compound	3	5	6 ·H ₂ O	8 ·H ₂ O	9	[H ₂ 10][ClO ₄] ₂ · CH ₃ CN
Formula	C ₄₂ H ₃₆ N ₆ O ₈	C ₂₄ H ₂₃ N ₃ O ₆	C ₂₂ H ₁₉ N ₃ O ₆ ·H ₂ O	C ₆ H ₁₄ N ₃ O· C ₈ H ₅ N ₂ O ₂ ·H ₂ O	C ₈ H ₆ N ₂ O ₂	[C ₄₈ H ₅₀ N ₆ O ₈]· [ClO ₄] ₂ ·CH ₃ CN
Formula Weight	752.77	449.5	439.4	323.4	162.2	1078.89
Lattice type	Triclinic	Triclinic	Monoclinic	Monoclinic	Monoclinic	Orthorhombic
Space group						
Symbol, No.	P $\bar{1}$, 2	P $\bar{1}$, 2	P2 ₁ /m, 11	P2 ₁ /c, 14	Cc, 9	Pnna, 52
Cell dimensions,						
a/Å	9.773(1)	9.134(2)	5.429(1)	15.118(2)	22.472(2)	24.886(5)
b/Å	11.755(1)	11.131(2)	22.306(5)	7.590(2)	13.931(2)	25.703(4)
c/Å	9.0341(8)	12.012(2)	9.276(2)	14.969(3)	7.093(2)	7.825(1)
α /deg	111.740(9)	64.48(2)	-	-	-	90
β /deg	94.236(9)	87.98(2)	93.35(2)	1123.89	101.49(1)	90
γ /deg	81.31(1)	85.52(2)	-	-	-	90
V/Å ³	952.8(2)	1098.7(4)	1121.4(5)	1570.4(5)	2176.0(6)	5005(2)
Z	1	2	2[a]	4	12[b]	4
F(000)	394	472	460	688	1008	2256
Radiation	Mo-K α	Cu-K α	Mo-K α	Cu-K α	Mo-K α	Cu-K α

Table 2. Cont.

μ/mm^{-1}	0.093	0.82	0.10	0.85	0.11	1.845
R_1	0.043	0.049	0.084	0.05	0.041	0.0886
wR_2	0.11	0.134	0.189	0.134	0.103	0.2283

[a] The molecule has crystallographic Cs symmetry.

[b] There are three crystallographically independent molecules in the asymmetric unit.

Preparation of dendrimer N,N,N',N'-tetrakis(2-(1,3-dioxo-1,3-dihydro-isoindol-2-yl)-ethyl)-1,2-ethyl-diamine (3).

Diphthalimidodiethylenetriamine (**4**) (0.8 mmol) (the preparation of which was described previously) [1-3] was dissolved in acetonitrile (100 mL), the mixture brought to reflux and then excess ethylene dibromide (28 mmol) and K_2CO_3 (0.9 mmol) were added. Reflux was continued for 5 days after which the mixture was filtered and the filtrate concentrated under reduced pressure (rotoevaporator) leaving a cream colored solid. The organic compounds were extracted with dichloromethane; the resulting mixture was filtered and then the filtrate allowed to evaporate slowly yielding cream colored crystals which were recrystallized from a dichloromethane/ethanol mixture (yield: *ca.* 58%); Anal. Calc. (%) for $\text{C}_{42}\text{H}_{36}\text{N}_6\text{O}_8$: C = 66.7, H = 4.7, N = 11.1; Found (%): C = 66.70, H = 4.79, N = 11.10. FAB MS (*m*-nitrobenzylalcohol): $m/z = 754$ (MH^+), 376 ($\text{M}-2\text{H}^{2+}$); IR: 1770 and 1653 cm^{-1} ; NMR δ_{H} (Brüker AC200 MHz, CDCl_3 , ppm): 2.6 (singlet, $-\text{CH}_2\text{CH}_2-$ bridging tertiary amine sites), 2.8 (triplet, $-\text{CH}_2-$ close to tertiary amine), 3.75 (triplet, $-\text{CH}_2-$ near phthalimide group), 7.75 (complex second order multiplet, aromatic C-H); δ_{C} : 35.4, 51.6, 52.2, 123.0, 132.2, 133.6 and 169.2.

{Bis-[2-(1,3-dioxo-1,3-dihydro-isoindol-2-yl)-ethyl]-amino}-acetic acid ethyl ester (5)

Compound **4** (0.1 mol), prepared as described previously [1-3], was dissolved in toluene (600 mL). anhydrous potassium carbonate (40g) and ethyl bromoacetate (15 mL) were then added and the mixture refluxed for two days. The resulting slurry was thoroughly washed with water and the toluene portion was then filtered to remove excess **4**; the filtrate was concentrated under vacuum to a thick oil, which was then dissolved in ethanol and crystallization allowed to proceed with reducing solvent volume. To the product, acetone was added till a clear solution was obtained and recrystallization was allowed to proceed with subsequent reduction in solvent volume (yield, *ca.* 40g, 65%); Anal. Calc. for $\text{C}_{24}\text{H}_{23}\text{N}_3\text{O}_6$: C = 64.14; H = 5.16; N = 9.35%; Found: C = 64.22; H = 5.15; N = 9.40%; NMR δ_{H} (200 MHz, CDCl_3 , ppm) 1.17-1.24 (t), 2.99 – 3.05 (t), 3.55 (t), 4.03 – 4.14 (q), 7.67 (s). The FAB MS of compound **5**, features peaks due to the monomer at $m/z = 450$ ($[\mathbf{5} + \text{H}]^+$) and dimers at $m/z = 899$ ($[\mathbf{5}_2 + \text{H}]^+$) (a peak due to a derivative of the dimer is also found at $m/z = 813$ ($[\mathbf{5}_2 - \text{CH}_2\text{COOCH}_2\text{CH}_3 + 2\text{H}]^+$). Loss of the non-phthalimide substituent is prevalent; thus a peak due to $[\mathbf{4} + \text{H}]^+$ is dominant.

{Bis-[2-(1,3-dioxo-1,3-dihydro-isoindol-2-yl)-ethyl]-aminium} acetate (6)

Compound **5** (1 mmol) obtained above was refluxed for 24 hours with NaOH (3 mmol) in a 1:2 ethanol-water solution (60 mL). To the resulting solution was added conc. HCl until the solution was acidic and then it was concentrated under vacuum. The resulting slurry was dissolved in water from which compound **6** crystallized as long needles (yield, 80%). Only monomer peaks are found in the FAB MS at $m/z = 422$ ($[\mathbf{6} + \text{H}]^+$), 444 ($[\mathbf{6} + \text{Na}]^+$) and 462 ($[\mathbf{6} + \text{Na} + \text{H}_2\text{O}]^+$); IR (cm^{-1}): 1775, 1705 and 1644; NMR δ_{H} (200 MHz, CDCl_3 , ppm): 2.8 (t); 3.4 (s); 3.7 (t); 7.7 (m); δ_{C} (200 MHz, CDCl_3 , ppm): 39.4; 55.2; 56.7; 138.1; 135.4; 126.9; 171.8; 176.1.

{(4-(2-Aminium-ethyl)-piperazin-2-one)(2-hydro-phthalazinate-1,4-dione)} (8)

Compound **5** (1 mmol) was refluxed overnight with hydrazine (3 mmol) in ethanol (60 mL). The resulting slurry was filtered and the filtrate concentrated under vacuum to give an oil which was dissolved in ethanol (*ca.* 20 mL) from which crystals of compound **8** were deposited at room temperature (yield, 60%); Anal. Calc. for $\mathbf{8} \cdot \text{H}_2\text{O}$ ($\text{C}_{14}\text{H}_{21}\text{N}_5\text{O}_4$): C = 52.00; H = 6.55; N = 21.66%; Found: C = 51.82; H = 6.61, N = 21.77%; NMR δ_{H} (200 MHz, CDCl_3 , ppm): 2.75 (m), 3.12 (t), 3.20 (s), 3.35 (t), 7.8-7.86(q), 8.05-8.10(q); δ_{C} : 39.01, 42.90, 50.26, 56.06, 57.64, 128.41, 131.62, 135.34, 163.69, 174.04; IR (cm^{-1}): 1551; 1594; 1643; FAB MS at (m/z): 144 (non-phthalimide moiety); 166(diprotonated phthalimide moiety); 287 (non-phthalimide dimer).

4-Hydroxy-2H-phthalazin-1-one (9)

Compound **5** (1 mmol) was refluxed for 24 hours with excess hydrazine (6 mmol); the resulting slurry was filtered and methanol added to the residue until it dissolved; upon reduction of solvent volume compound **9** crystallized as long needles (yield, 35%); NMR δ_{H} (200 MHz, CDCl_3 , ppm): 7.80-7.90 (q), 8.05-8.15 (q); δ_{C} : 128.52, 131.69, 135.48, 163.66, 188.63; IR (cm^{-1}): 1630; 1571. The filtrate yielded small quantities of compounds **6** and **7**.

Dendrimers N,N,N',N'-tetrakis(3-(1,3-dioxo-1,3-dihydroisoindol-2-yl)-propyl)-1,4-butanediamine (10), [4,17-bis(3-(1,3-dioxo-1,3-dihydroisoindol-2-yl)-propyl)-8,13-bis[3-[bis(3-aminopropyl)-amino]-propyl]-4,8,13,17-tetrazaeicosane-1,20-diamine] (11) and 1,4-diaminobutane[16]:(1,3-dioxo-1,3-dihydroisoindol-2-yl)-propylamine (12)

The corresponding dendritic amines (1 mmol) were refluxed with an excess of phthalic anhydride (4.4, 8.8 and 17.6 mmol for **10**, **11** and **12** respectively) in glacial acetic acid (50, 75 and 100 mL respectively). Reflux was prolonged (3, 7 and 13 days for **10**, **11** and **12** respectively) to enable all dendritic arms to react. The resulting brown oil was washed with potassium carbonate and extracted with a 3:2 chloroform-water mixture until the aqueous extract was neutral. The organic extract was dried over magnesium sulfate, concentrated under vacuum and the microcrystalline product dried under vacuum for 15 (**10**), 30 (**11**) or 45 (**12**) minutes; the yields were 92 (**10**), 79 (**11**) and 58 % (**12**),

respectively. Dendrimers **10** and **11** were obtained in pure form but it proved difficult to wash out all of the potassium carbonate and phthalate anions from the larger dendrimer **12**. Anal. Calc (%) for **11**: C = 57.5, H = 7.0, N = 9.0; Found C = 57.65, H = 6.85, N = 9.03. Mass spectrometry confirms molecular ion peaks at $m/z = 837$ (H10^+), 1814 (H11^+) and 3800 ($\text{H12}\cdot 2\text{H}_2\text{O}^+$). NMR δ_{H} (200 MHz, $(\text{CD}_3)_2\text{SO}$): 2.10 and 2.58 ($-\text{CH}_2-$) and ca. 7.8 (aromatic-H); IR revealed characteristic phthalimide bonds at 1700 and 1706 cm^{-1} . No peaks due to uncondensed N-H were found.

Compound $[\text{H}_2\mathbf{10}][\text{ClO}_4]_2\cdot 0.5\text{H}_2\text{O}$

Dendrimer **10** (0.1 g) in ethanol (75 mL) was acidified to pH 4-5 with perchloric acid and then evaporated off slowly at 50 °C to yield $[\text{H}_2\mathbf{10}][\text{ClO}_4]_2\cdot 0.5\text{H}_2\text{O}$ as colorless needles in 94% yield. The crystals were harvested and dried in tissue paper. Anal. Calc.(%) for $[\text{H}_2\mathbf{10}][\text{ClO}_4]_2\cdot 0.5\text{H}_2\text{O}$, C = 55.1, 4.9, N = 8.0; Found C = 55.08, H = 4.90, N = 8.01; IR revealed presence of phthalimide (1700 and 1706 cm^{-1}) and ClO_4^- (1100 cm^{-1}) functionalities; FAB MS featured a peak at $m/z = 935$ due to $[(\text{H}_2\mathbf{10})(\text{ClO}_4)]^+$ and at 837 for $[\text{H10}]^+$; NMR $^1\text{H}-^1\text{H}$ and $^1\text{H}-^{13}\text{C}$ connectivity studies (500 MHz, $(\text{CD}_3)_2\text{SO}$) confirmed the presence of $[\text{H}_2\mathbf{10}]^{2+}$. Crystals for X-ray analyses were grown in acetonitrile and obtained as $[\text{H}_2\mathbf{10}][\text{ClO}_4]_2\cdot \text{CH}_3\text{CN}$.

Lanthanide complexes of **10**

Better-defined products were obtained as follows. Lanthanide(III) nitrates (0.1 mmol) in ethanol (40 mL) was added dropwise, with continuous stirring, to **10** (0.3 mmol) in 1:1 ethanol-chloroform solution (50 mL) at 50 °C. The resulting solution was slowly evaporated off over three days and the product recovered in 90 - 93% yield by filtration. The products featured typical phthalimide IR bands at 1700 and 1706 cm^{-1} and NO_3^- at 1384, 1466 and 1320 cm^{-1} . Elemental analyses suggested a basic stoichiometry of $\text{Ln}(\mathbf{10})_2(\text{NO}_3)_3\cdot \text{solvent}$. Anal. Calc. (%) for $\text{Eu}(\mathbf{10})_2(\text{NO}_3)_3$: C = 57.3, H = 4.8, N = 10.4; Found, C = 57.01, H = 5.03, N = 10.32; Calc. for $\text{Gd}(\mathbf{10})_2(\text{NO}_3)_3\cdot \text{HNO}_3\cdot \text{H}_2\text{O}$: C = 54.1, H = 4.7, N = 10.9; Found, C = 54.17, H = 4.99, N = 10.98; Calc. for $\text{Tb}(\mathbf{10})_2(\text{NO}_3)_3\cdot \text{HNO}_3$: C = 55.4, H = 4.7, N = 10.8; Found, C = 55.40, H = 4.90, N = 10.87. Calc. for $\text{Y}(\mathbf{10})_2(\text{NO}_3)_3\cdot \text{HNO}_3\cdot 4\text{H}_2\text{O}$: C = 55.3, H = 5.1, N = 10.8; Found, C = 55.34, H = 4.92, N = 10.81.

Compounds $\text{Ln}_5(\text{H11})(\text{NO}_3)_{16}\cdot \text{solvent}$

A solution of lanthanide(III) nitrates (50 mL, 0.4 mmol) in ethanol (pH 5 - 6), was added dropwise to dendrimer **11** (0.05 mmol) in a 1:1 chloroform-ethanol mixture while stirring continuously. The compounds precipitated out as powders in 94 -96 % yield. Elemental analyses suggested a basic stoichiometry of $\text{Ln}_5(\text{H11})(\text{NO}_3)_{16}\cdot \text{solvent}$. Anal. Calc. (%) for $\text{La}_5(\text{H11})(\text{NO}_3)_{16}\cdot \text{CH}_3\text{CH}_2\text{OH}\cdot 12\text{H}_2\text{O}$: C = 33.5, H = 3.8, N = 11.1; Found, C = 33.42, H = 3.71, N = 10.74. Calc. for $\text{Eu}_5(\text{H11})(\text{NO}_3)_{16}\cdot 6\text{CH}_3\text{CH}_2\text{OH}$: C = 36.3, H = 3.9, N = 10.9; Found, C = 36.34, H = 3.96, N = 10.90.

Calc. for $\text{Gd}_5(\text{H11})(\text{NO}_3)_{16} \cdot 8\text{CH}_3\text{CH}_2\text{OH}$: C = 36.4, H = 4.1, N = 10.6; Found, C = 36.71, H = 3.97, N = 10.93; Calc. for $\text{Tb}_5(\text{H11})(\text{NO}_3)_{16} \cdot 10\text{H}_2\text{O}$: C = 33.0, H = 3.5, N = 11.1; Found, C = 33.29, H = 3.78, N = 10.93. The products featured typical phthalimide IR bands at 1700 and 1706 cm^{-1} and NO_3^- at 1384, 1466 and 1320 cm^{-1} .

Supplementary Material

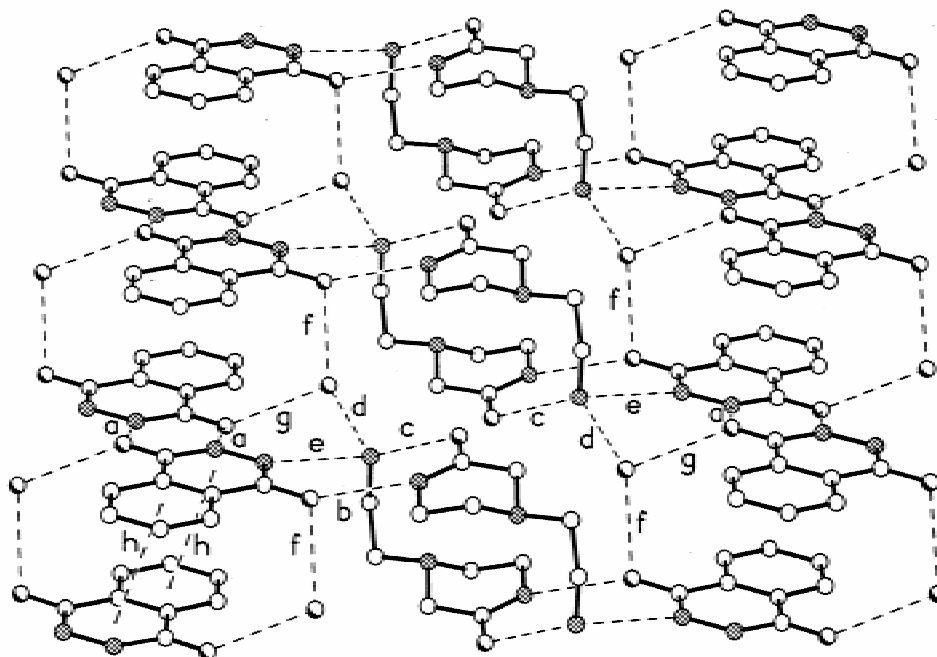


Figure S1. The supramolecular structure of **8** showing the step layers stabilized by $\pi \dots \pi$ stacks and hydrogen bonding.

Table S1. Hydrogen bonding geometries are respectively $\pi \dots \pi$ stacking (h) geometry: centroid-centroid distance 3.61 Å; mean interplanar separation 3.42 Å.

Bond (at atom):	[X...Y] and [H...Y] distances (Å); [X-H...Y] angle (°).		
a (N1):	2.81,	1.95,	159.
b (N11):	2.75,	1.94,	147.
c (N19):	2.90,	2.04,	160.
d (N19):	2.76,	1.95,	148.
e (N19):	2.90,	2.05,	157.
f (O20):	2.70,	1.80,	172.
g (O20):	2.81,	1.92,	174.

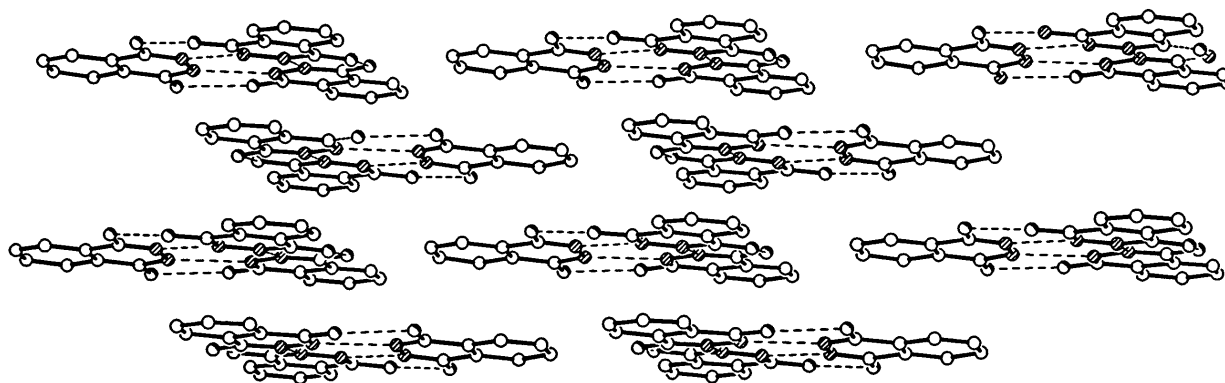


Figure S2. Supramolecular stacks of trimers of **9**.

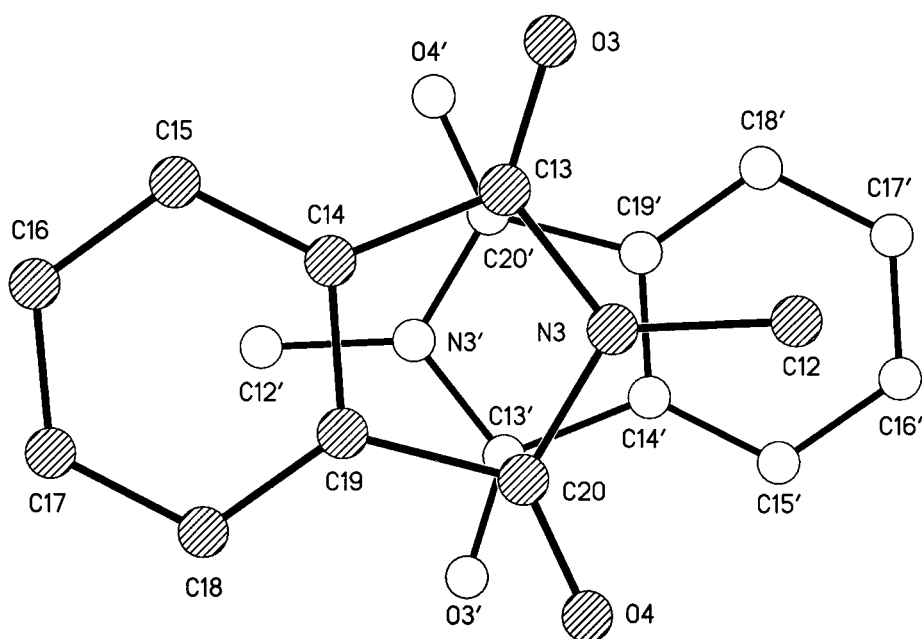


Figure S3. Plan view of the $\pi \cdots \pi$ stacking interaction of the phthalimido group of **3** containing N3.

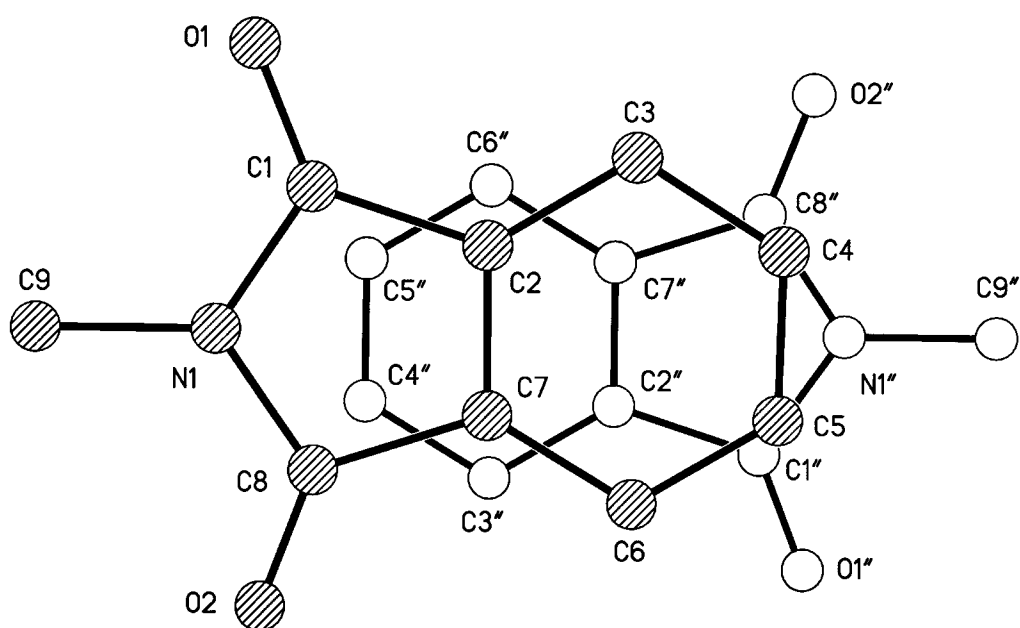


Figure S4. Plan view of the $\pi\cdots\pi$ stacking interaction of the phthalimido group of **3** containing N1.

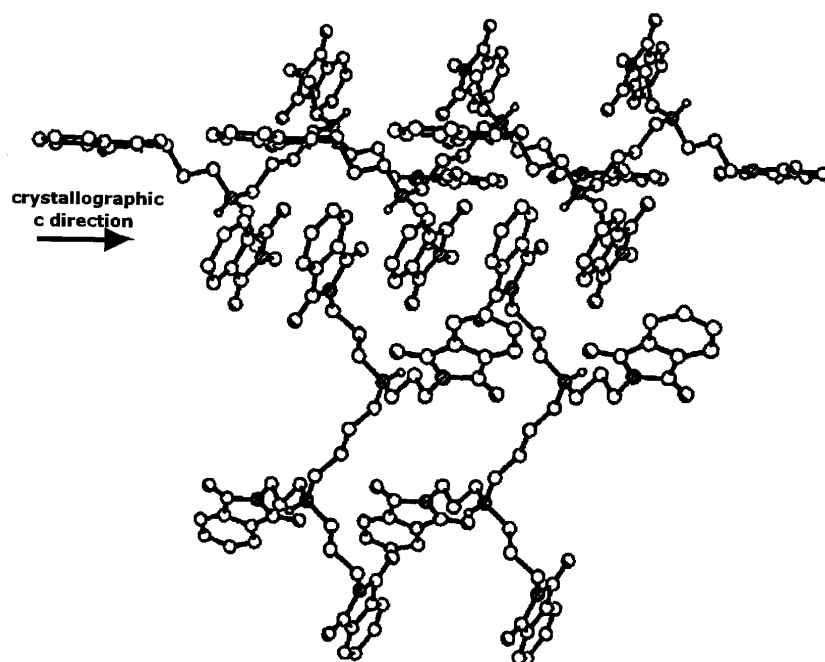


Figure S5. $\pi\cdots\pi$ stacking interactions along the crystallographic c-direction in $[\text{H}_2\mathbf{10}][\text{ClO}_4]_2 \cdot \text{CH}_3\text{CN}$

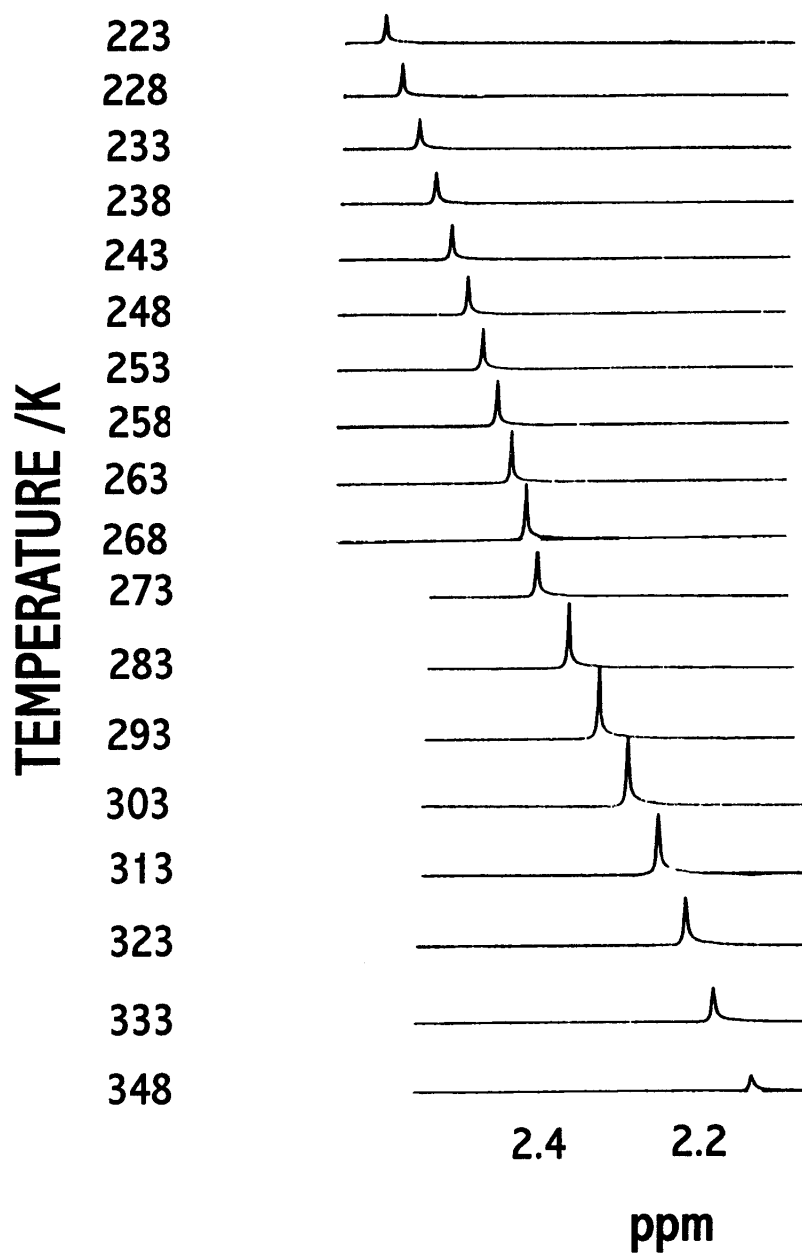


Figure S6. The temperature dependence of the ¹H-NMR chemical shifts of the NCH₂COO functionality of **5** in CD₃CN.

References and Notes

1. Barrett, D. M. Y.; Kahwa, I. A.; Mague, J. T.; McPherson, G. L. *J. Org. Chem.*, **1995**, *60*, 5946.
2. Barrett, D. M. Y.; Kahwa, I. A.; Williams, D. J. *Acta Crystallogr. Sect. C.*, **1996**, *52*, 2069.
3. Barrett, D. M. Y.; Kahwa, I. A.; Radüchel, B.; White, A. J. P.; Williams, D. J. *J. Chem. Soc. Perkin Trans. 2*, **1998**, 1851.

4. Silverstein, R. M.; Webster, F. X. *Spectrometric Identification of Organic Compounds, Sixth Edition*; John Wiley & Sons, Inc: New York, 1997; p. 174.
5. Gawronski, J.; Kazmierczak, F.; Growska, K.; Rychlewska, U.; Nordé, B.; Holmén, A. *J. Am. Chem. Soc.*, **1998**, *120*, 12083.
6. Hamilton, D. G.; Lynch, D. E.; Byriel, K. A.; Kennard, C. H. L. *Austr. J. Chem.*, **1997**, *50*, 439.
7. Hamilton, D. G.; Feeder, N.; Prodi, L.; Teat, S. J.; Clegg, W.; Sanders, J. K. M. *J. Am. Chem. Soc.*, **1998**, *120*, 1096
8. Schirling, D.; Decep, J. B.; Baltzer, S.; Pirion, F.; Wagner, J.; Hornperger, J. M.; Heydt, J. C.; Jung, M. J.; Danzin, C.; Weiss, R.; Fisher, J.; Mitshler, A.; De Cian, A. *J. Chem. Soc. Perkin Trans. 1*, **1992**, 1053
9. Jun-Li, T.; Ruan-Hua, D.; Yuen-Ping, L.; Zhong-Yuan, Z.; Li, L.; Kai-Bei, Y.; *Chinese J. Struct. Chem. (Jegon Huaxue)*, **1991**, *10*, 187.
10. Gajadhar-Plummer, A. S. Ph.D. Thesis, University of the West Indies, Mona, 1999.
11. (a) Barrett, D. M. Y. Ph.D. Thesis, University of the West Indies, Mona, 1997); (b) Howell, R. C. Ph.D. Thesis, University of the West Indies, Mona, 1997.
12. (a) Howell, R. C.; Kahwa, I. A.; White, A. J. P.; Williams, D. J. *J. Chem. Soc. Dalton Trans.*, **1996**, 961; (b) Howell, R. C.; Spence, K. V. N.; Kahwa, I. A.; Williams, D. J. *J. Chem. Soc. Dalton Trans.*, **1998**, 2727.
13. Williams, L. A. D.; Howell, R. C.; Young, R.; Kahwa, I. A. *Comparative Biochem. Physiol. Part C*, **2001**, *128*, 119.
14. (a) Latva, M.; Mäkinen, P.; Kulmala, S.; Haapakka, K. *J. Chem. Soc. Faraday Trans.*, **1996**, *92*, 3321; (b) Chen, J.; Selvin, P. R. *J. Am. Chem. Soc.*, **2000**, *122*, 657; (c) Fatin-Rouge, N.; Tóth, É.; Perret, D.; Backer, R. H.; Merbach, A. E.; Bünzli, J.-C. G. *J. Am. Chem. Soc.*, **2000**, *122*, 10810.
15. Bruce, J. I.; Parker, D.; Tozer, D. *Chem. Commun.*, **2000**, 2250.
16. (a) Bornhop, D. J.; Hubbard, D. S.; Houlne, M. P.; Adair, C.; Kiefer, G. E.; Pence, B.C.; Morgan, D. L. *Anal. Chem.*, **1999**, *71*, 2607; (b) Horrocks Jr, W. deW.; Bolender, J. P.; Smith, W.D.; Supkowski, R. M. *J. Am. Chem. Soc.*, **1997**, *119*, 5972.
17. (a) Aime, S.; Botta, M.; Fasano, M.; Terreno, E. *Chem. Soc. Rev.*, **1998**, *27*, 19; (b) Cohen, S. M.; Xu, J.; Radkov, E.; Raymond, K. N.; Botta, M.; Barge, A.; Aime, S. *Inorg. Chem.*, **2000**, *39*, 5747; (c) Ellison, J. J.; McMurry, T. J.; Lauffer, R. B. *Chem. Rev.*, **1999**, *99*, 2293.
18. (a) Zitha-Boven, E.; Elst, L. V.; Muller, R. N.; van Bekkum, H.; Peters, J. A. *Eur. J. Chem.* **2001**, 3101; (b) Merbach, A. E.; Tóth, É (Eds), *The Chemistry of Contrast Agents in Magnetic Resonance Imaging*; John Wiley: Chichester, U.K., 2001.
19. (a) Doyle, J. D.; Harriman, A.; Newport, G. L. *J. Chem. Soc. Perkin Trans. 2*, **1979**, 799; (b) Zenner, B.; Bender, M. L. *J. Am. Chem. Soc.*, **1961**, *83*, 2267.
20. (a) Epsetein, D. M.; Chappell, L. L.; Khalili, H.; Supkowski, R. M.; Horrocks Jr., W. deW.; Morrow, J. R. *Inorg. Chem.*, **2000**, *39*, 2130; (b) Gomez-Tangle, P.; Yatsimirsky, A. K. *J. Chem. Soc. Dalton Trans.*, **2001**, 2663; (c) Bligh, S. W. A.; Choi, N.; Evagorou, E. G.; McPartlin, M.; White, K. N. *J. Chem. Soc. Dalton Trans.*, **2001**, 3169

21. Thompson, M. K.; Vuchkov, M.; Kahwa, I. A. *Inorg. Chem.*, **2001**, *40*, 4332.
22. Schneider, H.-J. *Angew. Chem. Int. Ed. Engl.* **1991**, *30*, 1417.
23. (a) Ng, C. Y.; Motekaitis, R. J.; Martel, A. E. *Inorg. Chem.*, **1979**, *18*, 2982; (b) Buckingham, D. A.; Edwards, J. D.; McLaughlin, G. M. *Inorg. Chem.*, **1982**, *21*, 2770.
24. Kozlecki, T.; Samyn, C.R.; Alder, W.; Green, P. G. *J. Chem. Soc. Perkin Trans 2*, **2001**, 243.
25. Padies, H. H. *Ber. Bunsenges. Phys. Chem.*, **1992**, *96*, 1027.
26. Becker, D.; Botoshansky, M.; Gasper, N.; Herbstein, F. H.; Karni, M. *Acta Crystallogr. Sec.*, **1998**, *B54*, 671.
27. Gane, P. A.; Boles, M. O. *Acta Crystallogr.*, **1979**, *B35*, 2664
28. Isotopic abundance patterns were calculated with Isopro V 2.1 written by Yergey, J. A. Sheffield University (UK) and available at: [http://www.chem.schef.ac.uk/webelements.cgi\\$ isot](http://www.chem.schef.ac.uk/webelements.cgi$ isot).
29. Feeney, J.; Walker, S. M. *J. Chem. Soc. (A)*, **1966**, 1148.
30. Platas-Iglesias, C.; Piguet, C.; André, N.; Bünzli, J.-C. G. *J. Chem. Soc. Dalton Trans.*, **2001**, 3084.
31. Rigault S.; Piguet, C. *J. Am. Chem. Soc.*, **2001**, *122*, 9304.
32. (a) Dexter, L. *J. Chem. Phys.*, **1953**, *21*, 836; (b) Förster, Th. *Ann. Phys. (Leipzig)*, **1948**, *2*, 55.
33. (a) Newkome, G. R.; Moorefield, C. N.; Vögtle, F. *Dendritic Molecules Concepts, Synthesis, Perspectives*; VCH: Weinheim, Germany, 1996; (b) Newkome, G. R.; He, E.; Moorefield, C. W. *Chem. Rev.*, **1999**, *99*, 1689.
34. (a) Grayson, S. M.; Fréchet, J. M. *Chem. Rev.*, **2001**, *101*, 3819; (b) Zeng, F.; Zimmerman, S.C. *Chem. Rev.*, **1997**, *97*, 1681; (c) Astruc, F.; Chardac, F. *Chem. Rev.*, **2001**, *101*, 2991; (d) Bosman, A. W.; Janssen, H. M.; Meijer, E. W. *Chem. Rev.*, **1999**, *99*, 1665; (e) Schenning, J.; Meijer, E. W.; Bässler, H. *J. Phys. Chem. A.*, **2001**, *105*, 10220; (f) Meskers, S. C. J.; Bender, M.; Hübner, J.; Romanovskii, Yu. V.; Oestreich, M.; Weener, A. P. H. J.-W.; van Dongen, J. L. J.; Meijer, E. W. *J. Am. Chem. Soc.*, **1999**, *121*, 10346.
35. Tavakovic, I.; Miller, L. L.; Duan, R. G.; Tully, D. C.; Tomalia, D. C. *Chem. Mater.*, **1997**, *9*, 736.

Sample Availability: Samples of compounds **3**, **5**, **10** and **11** are available from the authors on request.